

**Tunneling, diffusion, and dissociation of Feshbach molecules in optical lattices**Taylor Bailey,<sup>1,\*</sup> Carlos A. Bertulani,<sup>1,†</sup> and Eddy Timmermans<sup>2,‡</sup><sup>1</sup>*Department of Physics and Astronomy, Texas A&M University-Commerce, Commerce, Texas 75429, USA*<sup>2</sup>*T-4, Los Alamos National Laboratory, Mail Stop B-262, Los Alamos, New Mexico 87545, USA*

(Received 8 November 2011; published 21 March 2012)

The quantum dynamics of an ultracold diatomic molecule tunneling and diffusing in a one-dimensional optical lattice exhibits unusual features. While it is known that the process of quantum tunneling through potential barriers can break up a bound-state molecule into a pair of dissociated atoms, interference and reassociation produce intricate patterns in the time-evolving site-dependent probability distribution for finding atoms and bound-state molecules. We find that the bound-state molecule is unusually resilient against break up at ultralow binding energy  $E_b$  ( $E_b$  much smaller than the barrier height of the lattice potential). After an initial transient, the bound-state molecule spreads with a width that grows as the square root of time. Surprisingly, the width of the probability of finding dissociated atoms does not increase with time as a power law.

DOI: [10.1103/PhysRevA.85.033627](https://doi.org/10.1103/PhysRevA.85.033627)

PACS number(s): 67.85.-d, 25.40.Lw, 24.50.+g, 26.20.-f

**I. INTRODUCTION**

Ultracold atoms in optical lattices provide a versatile tool for the experimental study of many-body quantum dynamics, with an unprecedented degree of accessibility [1]. Quantum many-body properties of cold atom gases such as Bose-Einstein condensates and ultracold fermions [2] are now studied in confining traps. Using the standing wave patterns of reflected laser beams, the ultracold atoms can experience a lattice potential of variable potential height [3], providing a laboratory for realizing the effective Hamiltonians of strongly coupled electron physics [4] and for studying tunneling physics [5]. Recent experiments have demonstrated that cold atom experimentalists can now observe individual atoms in an optical lattice with single site resolution [6]. The traps can realize systems of reduced dimensionality [7]. These developments allow for unparalleled tests of fundamental quantum dynamics such as quantum diffusion, interference, and localization in lattice potentials. In view of the condensed matter backdrop, the literature on transport phenomena of particles in periodic lattices found in crystals, quasicrystals, and metals is rich. Examples are Bloch oscillations of atoms due to the repeated Bragg scattering in tilted periodic potentials as reported in Ref. [8] and the shape of the quantum diffusion front in one-dimensional quasiperiodic systems studied in Ref. [9].

Combining the technique of Feshbach resonant [10] manipulation by tuning the strength of an external magnetic field [11], Grimm's group [12] succeeded in associating pairs of optical lattice atoms trapped at the same site into bound-state diatomic molecules of ultralow and tunable binding energy. In this paper, we investigate the dynamics of tunneling, diffusion, and tunneling-induced dissociation of ultracold diatomic molecules with a binding energy comparable to or smaller than the barrier height of the lattice potential. For quantum tunneling through a single barrier, composite particles are predicted to exhibit deviations from the exponential decay law. This quantum dynamics depends strongly on the intrinsic

(composite particle) structure as the binding energy decreases [13]. We study the diffusion of a Rydberg-like (with ultralow binding energy) molecule with fine-tuned binding energy in a one-dimensional periodic lattice. In the process of quantum tunneling through a barrier, the molecule can dissociate into a pair of atoms that experience the same lattice potential.

The tunneling, diffusion, and dissociation properties of composite particles in periodic lattices are subjects of increasing interest [14–16]. The combined quantum tunneling, interference, and dissociation can be used as a tool to prepare and exploit the properties of the intrinsic molecular structure and the population of bound and continuum states through the controlled diffusion of molecules in periodic potentials. The calculations reported in this article predict a universal behavior for the long-time evolution of the spreading width of molecular and atomic wave packets as they are affected by the reflection, tunneling, and diffusion process. Optical lattices are unique systems in this aspect, as they provide periodic barriers to study relevant quantum problems that no other known experimental setup can provide.

In Refs. [14–16], a treatment of molecular diffusion in one-dimensional optical lattices has been carried out. Instead of a “prepared” initial state, an exact bound-state solution is obtained for the same Hamiltonian used in our work. This approach contrasts with ours, where we use a molecular wave function in a uniform gas as the initial state. In principle, our results should agree in the limit of a tightly bound molecule, but it should be considered as an approximation for a weakly bound molecule. It is well-known that, when the initial bound state is not an exact eigenstate, the time evolution is affected. Thus, the conclusions drawn from our work are limited to the extent that only a prepared, localized, initial state is considered. A localized state has high energy components, which tend to facilitate tunneling and diffusion. We thus expect that our obtained tunneling and diffusion times are essentially larger than those obtained for an exact solution of the initial state for an optical lattice.

**II. TUNNELING AND DIFFUSION MODEL**

Our study is simplified on purpose, as we want to learn about the fundamental aspects of diffusion of composite objects,

\*taylor.chase.bailey@gmail.com

†carlos\_bertulani@tamu-commerce.edu

‡eddy@lanl.gov

subject to transforming transitions from bound to continuum states. The optical lattice potential has the form of a sine function with a periodicity that is the lattice constant  $D$ , equal to half the wavelength of the interfering laser, giving  $D = 0.2\text{--}5\ \mu\text{m}$  (the longer wavelengths are accessible with a carbon dioxide laser, for instance). Experimentally, the binding energy of a Feshbach molecule is tuned up by a magnetic field  $B$  that controls the scattering length  $a$ . This length varies with the magnetic field strength  $B$  as

$$a = a_{\text{bg}} \left[ 1 - \frac{\Delta}{(B - B_0)} \right], \quad (1)$$

where  $a_{\text{bg}}$  denotes the background scattering length, i.e., the value of the scattering length far from resonance.  $B_0$  represents the on-resonance magnetic field, and  $\Delta$  is the resonance width. For most known resonances,  $\Delta$  takes on a value between 1 mG and 10 G. The scattering length  $a$  can be varied from  $a_{\text{bg}} \sim \text{nm}$  to several micrometers [17]. Near the resonance, the binding energy of the binary system of reduced mass  $\mu$  and scattering length  $a$  are related by  $E_b = \hbar^2/\mu a^2$ , so that

$$\nu_b = \frac{E_b}{h} = \frac{h}{4\pi^2\mu a^2}. \quad (2)$$

For diatomic rubidium-87 molecules,  $\mu = Am_N/2$ , where  $m_N$  is the nucleon mass and the atomic number  $A = 87$ . The numerical value of the constant of circulation  $h/m$  is equal to  $h/m = 8.0/(A/100)\ \mu\text{m}^2/\text{ms}$ , and the binding frequency is

$$\nu_b = \frac{1}{(\pi^2 A/100)} \frac{\text{kHz}}{(a/\mu\text{m})^2}. \quad (3)$$

Thus, for  $a \sim 10\ \text{nm}$  and larger, typical binding energies are of the order of MHz, although very close to the resonance a binding energy of a few Hz can be achieved [18]. We use binding energies in the range of kHz to study the dissociation and diffusion dependence on the molecule binding.

We consider a molecule consisting of two identical rubidium-87 atoms. The Hamiltonian for the system interacting with the optical lattice is given by  $H = T_1 + T_2 + V_1 + V_2 + v$ , where  $T_i$  is the kinetic energy of atom  $i$ ,  $V_i$  is the periodic potential of the lattice, given by

$$V_i = V_0 \left[ 1 - \cos\left(\frac{\pi x_i}{D}\right) \right], \quad (4)$$

and  $v$  is the interaction potential between the atoms. The position of each atom within the lattice is given by  $x_i$  and  $\mu = m_{\text{Rb}}/2$  is the reduced mass of the diatomic system. The interatom potential is assumed to be governed by the magnetic field near a Feshbach resonance, which is directly related to a positive scattering length  $a$ . As we only consider a single bound state regulated by the scattering length, we assume a Dirac- $\delta$  potential of the form  $v(x_{12}) = -(2\pi\hbar^2/\mu a)\delta(x_{12})$ , where  $x_{12} = x_1 - x_2$ . This potential holds a bound state at energy  $E_b = -\hbar^2/2\mu a^2$  with wave function

$$\psi(x_{12}) = \sqrt{k} \exp(-k|x_{12}|), \quad \text{with } k = \sqrt{-2\mu E_b/\hbar^2}. \quad (5)$$

After preparing the initial state with a bound-state molecule localized within one of the lattice sites, we calculate the tunneling, diffusion, and dissociation properties of the Feshbach molecule. Taking the center of the initially occupied lattice site as the origin, the initial wave function is written as  $\Psi_0(x, y) = \psi(x_{12})\Phi(x_s)$ , where  $x_s = (x_1 + x_2)/2$  is the center of mass of the molecule, and

$$\Phi(x_s) = \frac{1}{(2\pi\sigma_0^2)^{1/4}} \exp\left[-\frac{x_s^2}{4\sigma_0^2}\right] \quad (6)$$

is a normalized Gaussian wave packet centered on the origin and localized with initial width  $\sigma_0$ .

We calculate the wave function of the two atoms in a spatial grid for the  $x_1$  and  $x_2$  coordinates, so that  $x_i^{(j)} = j\Delta x$ , with  $j = 1, 2, \dots, N$ . The wave function  $\Psi(x_1, x_2, t)$  is represented by the finite set of time-dependent functions  $\Psi(x_1^{(i)}, x_2^{(j)}, t) = \Psi_{jk}(t)$  at the points  $(x_1^{(i)}, x_2^{(j)})$  of the spatial grid. The derivations in the kinetic operators of the Hamiltonian are approximated by three-point formulas. For the boundary conditions on the far left or far right of the grid we set  $\Psi_{j0} = \Psi_{jN} = \Psi_{0k} = \Psi_{Nk} = 0$ .

The time evolution of the molecule wave function  $\Psi(x_1, x_2, t)$  is obtained by solving the Schrödinger equation by a finite difference method. The wave function  $\Psi(t + \Delta t)$  at time  $t + \Delta t$  can be calculated from the wave function at time  $t$ ,  $\Psi(t)$ , by applying the unitary time evolution operator,  $\mathbf{U}$ . In matrix notation for coordinates  $(x, y)$ ,

$$\Psi(t + \Delta t) = \mathbf{U}(t + \Delta t, t)\Psi(t). \quad (7)$$

For a small time step  $\Delta t$  between iterations, the time evolution operator can be approximated as

$$\mathbf{U}(t + \Delta t, t) \simeq \frac{1 + (\Delta t/2i\hbar) H(t)}{1 - (\Delta t/2i\hbar) H(t)}. \quad (8)$$

This is an implicit equation for the time evolution and is correct up to and including terms of the order  $(\Delta t)^2$ . It requires carrying out matrix multiplications and inversions at each iteration. The inversion is performed by an extension of the Peaceman-Rachford method and is well documented in the literature [19,20].

To analyze the time-evolving two-particle wave function  $\Psi$ , it is useful to distinguish the bound-state molecule amplitude from that of dissociated atoms. The bound-state molecule is associated with the projection of the two-particle wave function on the bound-state wave function  $\psi$  of Eq. (5). The probability of finding a bound-state molecule in the interval  $(x_s - dx_s/2, x_s + dx_s/2)$  at time  $t$  is  $P_M(x_s, t)dx_s$ , where

$$P_M(x_s, t) = \left| \int dx_{12} \Psi(x_s - x_{12}/2, x_s + x_{12}/2, t) \psi^*(x_{12}) \right|^2. \quad (9)$$

The probability of finding a dissociated atom is the difference of two probabilities: the probability of finding an atom and the probability that this atom is part of a bound-state molecule. We refer to the probability of finding a dissociated atom within an interval  $(x - dx/2, x + dx/2)$  at time  $t$  as  $P_A(x, t)dx$ . As this atom can be either atom 1 or atom 2, and as we have to subtract

out the bound molecule probability, we obtain

$$P_A(x,t) = \int dx_2 |\Psi(x, x_2, t)|^2 - \left| \int dx_2 \Psi(x, x_2, t) \psi^*(x - x_2) \right|^2 + \int dx_1 |\Psi(x_1, x, t)|^2 - \left| \int dx_1 \Psi(x_1, x, t) \psi^*(x_1 - x) \right|^2. \quad (10)$$

In accordance with intuition—the dissociation of each molecule (in a statistical ensemble) produces two atoms; Eqs. (9) and (10) ensure that

$$\int dx \left[ P_M(x,t) + \frac{P_A(x,t)}{2} \right] = \int dx_1 \int dx_2 |\Psi(x_1, x_2, t)|^2 = 1, \quad (11)$$

corresponding to a normalization condition satisfied by the atom or molecule probabilities.

### III. RESULTS AND DISCUSSION

We first consider the case of a tightly bound molecule for which little dissociation occurs. There is no coupling to the continuum,  $P_A = 0$ , and the  $P_M$  probability of a bound-state molecule diffuses as a single particle in a quantum tunneling and diffusion process in the periodic potential. An illustrative example of  $P_M(x,t)$  is shown in Fig. 1. The lattice constant  $D$  of the potential is equal to  $D = 2 \mu\text{m}$  and the binding energy  $E_b$  of the bound-state molecule is given by  $E_b = 10 \text{ kHz}$ . The potential barrier height  $V_0$  and the width are chosen so that the molecule can easily tunnel through the barriers,  $V_0 = 200 \text{ Hz}$ . The graphs show the probability of finding a molecule at position  $x$  after time  $t = 0$ ,  $t = 10 \text{ ms}$ ,  $t = 25 \text{ ms}$ , and  $t = 100 \text{ ms}$ . For better visualization the barrier height is rescaled by a factor so that the height of the particle probability at the central position matches with the top of the barrier. As expected, due to the exponential decay of the wave function within the barriers, the probability distribution peaks in the middle of the lattice sites. The initial wave packet, localized at the origin, leaks successively through each barrier. The interference of scattered and transmitted waves induces an increasing number of wave fronts to appear in the probability distribution as time evolves. The width of the probability distribution for finding a bound-state molecule grows with increasing time. As a consequence of the mirror symmetry of the initial state and the Hamiltonian, the distribution function maintains mirror symmetry.

In Fig. 2 we show the time dependence of the escape probability—the probability that the molecule is not found in the initial lattice site—of the strongly bound rubidium molecules of the previous calculation. The time dependence is plotted as a function of increasing potential barrier heights. The barrier height increases each time by a factor of 1.5 in going from the solid ( $V_0 = 200 \text{ Hz}$ ) to the dashed-dotted curve, from the dashed-dotted to the long-dashed curve, and from the long-dashed to the dotted curve. As expected, the escape probability increases at a slower pace if the barrier height is larger. After reaching a maximum value the escape probability

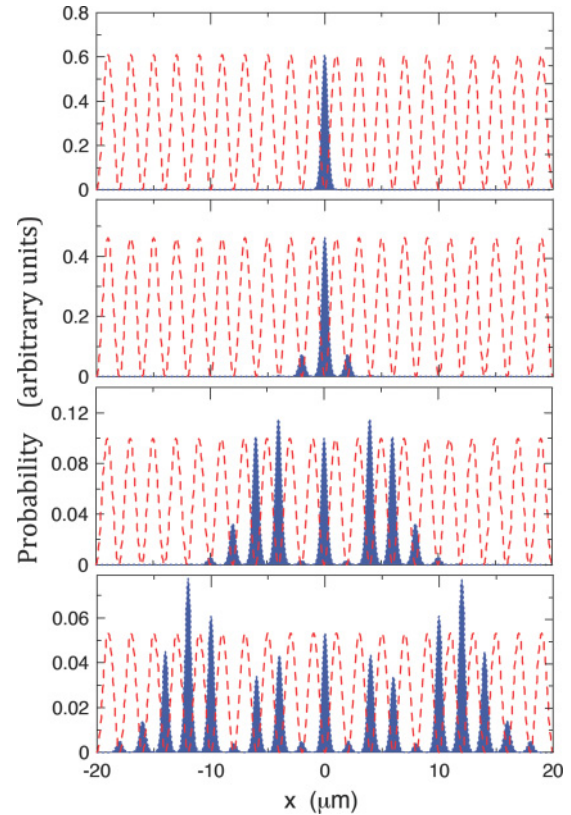


FIG. 1. (Color online) Time evolution of the probability distribution of strongly bound ( $E_b = 10 \text{ kHz}$ ) rubidium molecules in an optical lattice with size  $D = 2 \mu\text{m}$ . From top to bottom the time is  $t = 0$ ,  $t = 10 \text{ ms}$ ,  $t = 25 \text{ ms}$ , and  $t = 100 \text{ ms}$ , respectively.

oscillates due to reflections that feed back amplitude to the initial position.

We now consider the quantum diffusion of Rydberg molecules with low binding energy  $E_b$ , where  $E_b < V_0$ . In this regime, a molecule does not only diffuse by quantum tunneling through the barriers of the lattice, but can also dissociate into a pair of atoms in the process of tunneling and  $P_A \neq 0$ . Many notable examples of this physics with a single potential barrier

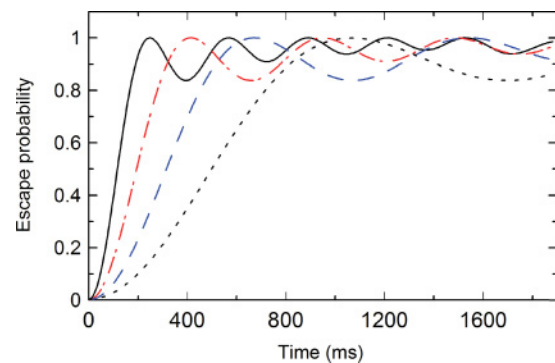


FIG. 2. (Color online) Time dependence of the escape probability of strongly bound rubidium molecules from an optical lattice with size  $D = 2 \mu\text{m}$ , as a function of increasing potential barrier heights. The barrier height increases each time by a factor of 1.5 in going from the solid to the dashed-dotted curve, from the dashed-dotted to the long-dashed curve, and from the long-dashed to the dotted curve.

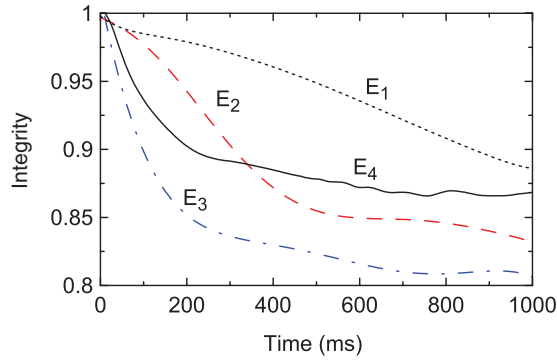


FIG. 3. (Color online) Time dependence of the “integrity” probability of loosely bound rubidium molecules by tunneling and diffusion through an optical lattice with lattice constant  $D = 2 \mu\text{m}$  and potential barrier height  $V_0 = 5 \text{ kHz}$ . The integrity is the probability that the molecule remains in its bound state. The binding energies were parametrized in terms of the barrier height, with  $E_4 = V_0/20$ ,  $E_3 = V_0/5$ ,  $E_2 = V_0/2$ , and  $E_1 = V_0/1.2$ .

occur in nuclear fusion reactions (see, e.g., Refs. [13,21]). The probability that the atoms remain bound in the initial molecule state,  $\int dx P_M(x,t)$ , is called the “integrity.” In Fig. 3 we plot the time dependence of the integrity probability of rubidium molecules as they tunnel and diffuse through an optical lattice with size  $D = 2 \mu\text{m}$  and a fixed potential barrier height  $V_0 = 5 \text{ kHz}$ . The binding energies were parametrized in terms of the barrier height, with  $E_4 = V_0/20$ ,  $E_3 = V_0/5$ ,  $E_2 = V_0/2$ , and  $E_1 = V_0/1.2$ . While the center of mass of the two atoms is initially localized within a few micrometers, the atom or molecule probabilities spread over time. It is necessary to have a sufficiently large lattice to accommodate the  $P_A$  and  $P_M$  probabilities. This is relatively easily achieved in one-dimensional calculations, but represents a computational challenge for calculations in higher dimensions. In some cases we work with a spatial mesh encompassing a few hundred lattice sites to allow for convergence of the loosely bound molecule amplitude.

As the binding energy of the molecules decreases from  $V_0$ , the integrity probability initially reduces. In this regime, the tunneling rate increases with lower binding energy and tunneling favors dissociation, in line with previous studies in fusion reactions [13,21]. The natural interpretation is that increased tunneling also increases the interactions of the individual atoms with a larger number of barriers, thus increasing the dissociation probability.

Despite the apparently obvious interpretation given above, the molecule is also resilient to breakup: even at the smallest binding value, the breakup probability is not that big. This interpretation loses meaning at very low binding energies, as seen by the case of  $E_4 = V_0/20$ , in which case the integrity increases relative to that of cases 2 and 3 of higher binding energy. At that binding energy, the trend is reversed and the molecule tends to remain intact. This result is not unusual, as other tunneling systems exhibit similar behavior. Perhaps the most familiar example is the tunneling of a Cooper pair [22]. The pair does not usually dissociate as it tunnels through a barrier. However composite particles may dissociate as the particles tunnel through multiple barriers, as in the case of a

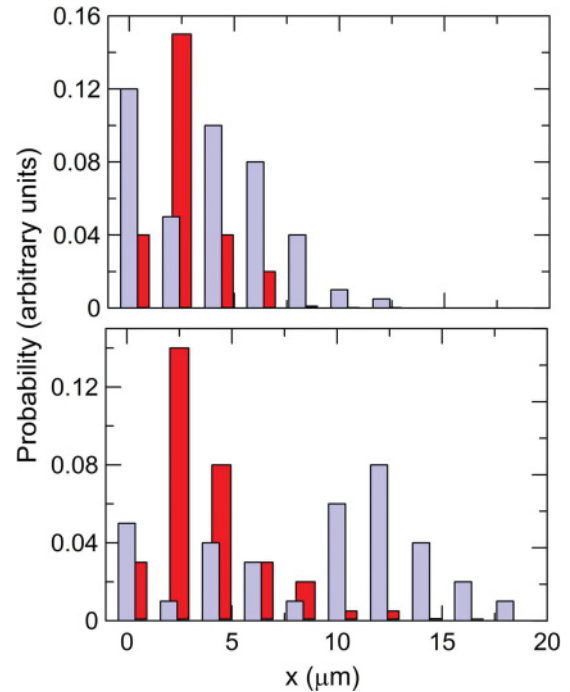


FIG. 4. (Color online) Lattice diffusion of molecules. The hatched histograms are the relative probability of finding a molecule in its ground state at a given position along the lattice. The solid histograms give the relative probability of finding individual atoms after the dissociation. This figure was generated for the highest dissociation probability (20%) described in Fig. 3.

lattice potential. Moreover, the binding mechanism of a Cooper pair is rather different from the interparticle potential binding considered here.

In Fig. 4 we show the probability of finding the bound-state molecule (hatched histograms) or of finding a dissociated atom (solid histograms) in the different lattice sites for the case  $E_b = 250 \text{ kHz}$  and  $V_0 = 5 \text{ kHz}$  at two different times,  $t_1 = 200 \text{ ms}$  and  $t_2 = 400 \text{ ms}$ . The time progression gives a sense of the quantum dynamics. The height of the hatched (bound molecule) histogram for site  $i$ ,  $P_{M,i}$ , is equal to  $P_{M,i} = \int_{|i-1/2|D}^{[i+1/2]D} dx P_M(x)$ , whereas the height of the solid (dissociated atom) histogram,  $P_{A,i}$ , gives the value of  $P_{A,i} = \int_{|i-1/2|D}^{[i+1/2]D} dx P_A(x)$ . Note that the diffusion front of the bound-state molecule spreads with a speed greater than that of the dissociated atoms. Because it takes additional time for the molecules to dissociate, the atoms diffuse slower than the bound-state molecules within the lattice.

It takes time for the molecules to dissociate and additional time for the atoms to diffuse after the dissociation. We thus predict that the molecules, initially confined within a lattice site, will tunnel and diffuse away from the initial position at a speed higher than that of the atoms that are created in the dissociation of the molecules.

We can characterize the speed of the wave front progression for bound-state molecule diffusion in the lattice by calculating the width  $\sigma(t) \equiv \sqrt{\langle r^2(t) \rangle}$ , where the average is taken with respect to the bound-state molecule distribution, when characterizing the bound-state molecule diffusion,  $\sigma_M(t) \equiv$



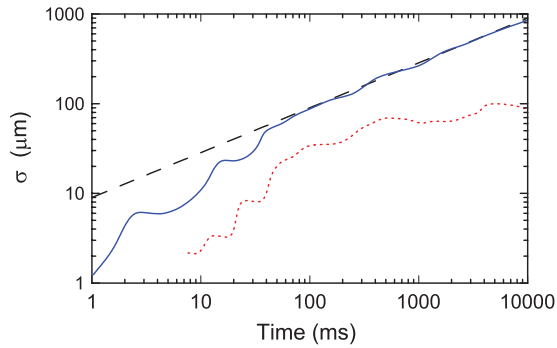


FIG. 5. (Color online) Time dependence of the spreading width of bound molecules,  $\sigma_M(t)$ , shown by the solid line, and of dissociated atoms,  $\sigma_A(t)$ , shown by the dotted line, defined in the text. The dashed curve is a fit of the asymptotic time dependence with the analytical formula, Eq. (15).

$\sqrt{\int dx x^2 P_M(x,t) / \int dx P_M(x)}$ , and with respect to the dissociated atom spreading when characterizing the dissociated atom spreading,  $\sigma_A(t) \equiv \sqrt{\int dx x^2 P_A(x,t) / \int dx P_A(x)}$ . In the long-time regime, the molecule and atom distributions do not spread as fast as the probability of a single free particle quantum wave function does,  $\sigma_{\text{free}} \sim \hbar t / (2M\sigma_0)$ , where  $M$  is the mass of the particle and  $\sigma_0$  is the initial width of the wave packet. In contrast, the distribution of the bound-state molecule with low binding energy spreads as  $\sigma_M(t) \sim t^{1/2}$  at long times, as shown in Fig. 5). The dissociated atoms spread more slowly still, although their width, shown by the dotted line, does not attain the form of a power law in time. Instead, the width appears to grow in steps becoming orders of magnitude smaller than the molecule width at long times. We also find a nontrivial correlation between  $\sigma_A(t)$  and the molecule binding energy. Generally, molecules of lower binding energy exhibit a more complex time dependence of  $\sigma_A$  upon  $t$ .

#### IV. CONCLUSIONS

The long-time power scaling  $\sigma_M \sim t^{1/2}$  contrasts with the linear scaling of a free particle wave packet and of a Gaussian wave packet propagating in a tight-binding model Hamiltonian [23,24] (if the lattice potential is not tilted). How can we understand the scaling of  $\sigma_M$ ? We can try to understand the long-time particle diffusion through the lattice by using semiclassical arguments. Starting from the time-dependent Schrödinger equation  $i\hbar\partial_t\phi = -\hbar^2\partial_x^2\psi/2m + V\psi$ , where  $V$  is the lattice potential, and writing the wave function as  $\psi = \sqrt{\rho}\exp(iS/\hbar)$ , we get the semiclassical equation

$$m\frac{\partial v}{\partial t} + mv\frac{\partial v}{\partial x} = -\frac{\partial(V+U)}{\partial x}, \quad (12)$$

where  $v = \partial_x S/m$  is the measure of the particle velocity and

$$U = -\hbar^2\frac{1}{2m\sqrt{\rho}}\frac{\partial^2\sqrt{\rho}}{\partial x^2} \quad (13)$$

represents the Bohm quantum potential [25].

Tunneling of a wave packet through a sequence of barriers effectively slows down the wave-packet spreading and the process becomes akin to quantum diffusion. Our numerical

results can be simulated by adding a friction term,  $bv$ , on the left-hand side of the semiclassical equation (12), with  $b$  being a friction constant.

Inserting  $\rho = \psi^*\psi$  for the wave packet, Eq. (6), and allowing a time-dependent width,  $\sigma(t)$ , we obtain

$$m\frac{\partial^2\sigma}{\partial t^2} + b\frac{\partial\sigma}{\partial t} = \frac{\hbar^2}{4m\sigma^3} - \left\langle \frac{\partial V}{\partial x} \right\rangle, \quad (14)$$

where the last term contains an average with respect to the wave packet. For a periodic potential and large values of  $\sigma$ , this term averages to zero ( $\langle \partial V / \partial x \rangle = 0$ ) and  $\sigma(t)$  can be obtained by solving Eq. (14) for a general case, subject to the initial condition that  $\sigma(t=0) = \sigma_0$ .

There is a competition between the first and second derivatives on the left-hand side of Eq. (14). One strategy to find the asymptotic time dependence of  $\sigma(t)$  is to solve Eq. (14) neglecting one of the partial derivatives in different regimes and finding the value for which both solutions match. This procedure is validated by comparing to the numerical solutions of Eq. (14) for different sets of values of  $m$ ,  $b$ , and  $\sigma_0$ . The calculations show that after a transient time, and for a strongly bound molecule, the approximate result holds,

$$\sigma(t) \simeq 0.31 \left( \frac{\hbar^2 t}{mb\sigma_0^2} \right)^{1/2}, \quad (15)$$

where  $m$  is the mass of the molecule. This asymptotic behavior is shown in Fig. 5.

Defining a diffusion coefficient by means of  $D_d = \partial_t \sigma^2 / 2$  yields

$$D_d \sim 0.156 \frac{\hbar^2}{mb\sigma_0^2}. \quad (16)$$

Note the difference with the classical Einstein diffusion constant,  $D_d = kT/b$ . We argue that the effective ‘‘temperature’’ of this system is the kinetic energy of the initial state,  $T \propto \hbar^2/m\sigma_0^2$ . The dependence of the temperature, or diffusion coefficient, on the initial kinetic energy is a new result to be tested experimentally. Notice, however, that these results might not hold when molecules interact among themselves.

For the dissociated molecules or atoms, the time dependence of the spreading width of the atoms within the lattice is not well fitted by any power-law dependence on time (dotted curve in Fig. 4). We observe a nontrivial correlation between  $\sigma_{\text{atoms}}(t)$  and the molecule binding energy.

Currently, many of the optical lattice descriptions are based on the Bose-Hubbard Hamiltonian [26], which is a tight-binding model. This Hamiltonian is familiar from strongly correlated systems and conveniently describes atom-atom interactions in many-atom systems. In addition, however, recent Feshbach resonance experiments in optical lattices call for the description of bound-state molecule dynamics, including the diffusion by tunneling of atoms and molecules as well as the dissociation of molecules into atoms. In this work we have shown that the dissociation followed by tunneling of individual atoms gives rise to a complex dynamics, parts of which cannot be described by power-law scaling at large times. This part requires additional theory follow-up. In our simple model based on solving the time-dependent Schrödinger

equation on a space-time lattice, we obtain fruitful insights into this dynamics. Some unexpected features, such as the weakening of dissociation as the binding energies decrease or the robustness of the molecule that tends to tunnel as a single compact object, are exhibited by the numerical results. We have also observed that the asymptotic time behavior of the spreading width of the molecules is amenable to an analytical treatment. A simple power law,  $\sigma \propto t^{1/2}$ , seems to arise from the numerical solutions. The diffusion of molecules and their dissociation during tunneling is a rich phenomenon which certainly deserves more research. The inclusion of interactions

between the molecules, and atoms, in the dynamics of diffusion is also of great interest.

#### ACKNOWLEDGMENTS

This work was partially supported by the US Department of Energy under Grants No. DE-FG02-08ER41533 and No. DE-FC02-07ER41457 (UNEDF, SciDAC-2) and the US National Science Foundation under Grant No. PHY-0855082. The work of E.T. was supported by the Los Alamos Laboratory Directed Research and Development (LDRD) Program.

- 
- [1] M. Lewenstein and W. Vincent Liu, *Nature Physics* **7**, 101 (2011).
- [2] I. Bloch, J. Dalibard, and W. Zwerger, *Rev. Mod. Phys.* **80**, 885 (2008).
- [3] M. Greiner and S. Fölling, *Nature (London)* **453**, 736 (2008).
- [4] S. Sachdev, *Nat. Phys.* **4**, 173 (2008).
- [5] E. Arimondo and S. Wimberger, e-print [arXiv:1104.2535](https://arxiv.org/abs/1104.2535).
- [6] W. Bakr, J. Gillen, A. Peng, S. Fölling, and M. Greiner, *Nature (London)* **462**, 74 (2009); J. Sherson, C. Weitenberg, M. Endres, M. Cheneau, I. Bloch, and S. Kuhr, *ibid.* **467**, 68 (2010); W. Bakr, A. Peng, M. Tai, R. Ma, J. Simon, J. Gillen, S. Fölling, L. Pollet, and M. Greiner, *Science* **329**, 547 (2010); C.-L. Hung, X. Zhang, N. Gemelke, and C. Chin, *Phys. Rev. Lett.* **104**, 160403 (2010).
- [7] A. Görlitz *et al.*, *Phys. Rev. Lett.* **87**, 130402 (2001).
- [8] M. Ben Dahan, E. Peik, J. Reichel, Y. Castin, and C. Salomon, *Phys. Rev. Lett.* **76**, 4508 (1996).
- [9] J. Zhong, R. B. Diener, D. A. Steck, W. H. Oskay, M. G. Raizen, E. W. Plummer, Z. Zhang, and Q. Niu, *Phys. Rev. Lett.* **86**, 2485 (2001).
- [10] H. Feshbach, *Ann. Phys. (NY)* **5**, 357 (1958).
- [11] C. Chin, R. Grimm, and P. Julienne, *Rev. Mod. Phys.* **82**, 1225 (2010).
- [12] G. Thalhammer, K. Winkler, F. Lang, S. Schmid, R. Grimm, and J. Hecker Denschlag, *Phys. Rev. Lett.* **96**, 050402 (2006).
- [13] C. A. Bertulani, V. V. Flambaum, and V. G. Zelevinsky, *J. Phys. G* **34**, 2289 (2007).
- [14] G. Orso, L. P. Pitaevskii, S. Stringari, and M. Wouters, *Phys. Rev. Lett.* **95**, 060402 (2005).
- [15] M. Wouters and G. Orso, *Phys. Rev. A* **73**, 012707 (2006).
- [16] Y. Ohashi, *Phys. Rev. A* **78**, 063617 (2008).
- [17] E. A. Donley *et al.*, *Nature (London)* **412**, 295 (2001).
- [18] R. V. Krems, W. C. Stwalley, and B. Friedrich, eds., *Cold Molecules: Theory, Experiment, Applications* (CRC Press, Boca Raton, FL, 2009).
- [19] R. S. Varga, *Matrix Iterative Analysis* (Prentice Hall, Englewood Cliffs, NJ, 1962).
- [20] W. H. Press, S. A. Teukolsky, W. T. Vetterling, and B. P. Flannery, *Numerical Recipes: The Art of Scientific Computing*, 3rd ed. (Cambridge University Press, Cambridge, UK, 2007).
- [21] C. A. Bertulani, e-print [arXiv:1105.6356](https://arxiv.org/abs/1105.6356).
- [22] A. M. v. d. Brink, A. A. Odintsov, P. A. Bobbert, and G. Schn, *Z. Phys. B* **85**, 459 (1991).
- [23] H. J. Korsch and S. Mossmann, *Phys. Lett. A* **317**, 54 (2003).
- [24] A. Klumpp, D. Witthaut, and H. J. Korsch, *J. Phys. A: Math. Theor.* **40**, 2299 (2007).
- [25] D. Bohm, *Phys. Rev.* **85**, 166 (1952).
- [26] D. Jaksch, C. Bruder, J. I. Cirac, C. W. Gardiner, and P. Zoller, *Phys. Rev. Lett.* **81**, 3108 (1998).